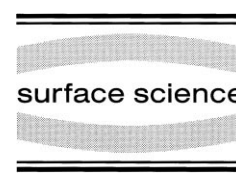




ELSEVIER

Surface Science 454–456 (2000) 88–93



www.elsevier.nl/locate/susc

## Electronic structure of a catalyst poison: Br/Pt(110)

A. Menzel<sup>a</sup>, K. Swamy<sup>a</sup>, R. Beer<sup>a</sup>, P. Hanesch<sup>a,1</sup>, E. Bertel<sup>a,\*</sup>, U. Birkenheuer<sup>b</sup>

<sup>a</sup> *Institute of Physical Chemistry, University of Innsbruck, A-6020 Innsbruck, Austria*

<sup>b</sup> *Lehrstuhl für Theoretische Chemie, TU München, Munich, Germany*

### Abstract

The system Br/Pt(110) is studied by scanning tunneling microscopy, low energy electron diffraction, angle resolved photoemission and self-consistent ab initio calculations. Bromine is molecularly adsorbed at 300 K, but dissociates at  $T > 400$  K. The Br atoms adsorb substitutionally and form quasi-one-dimensional (1D) Pt–Br–Pt chains. The 1D character of the chains gives rise to a charge density wave ground state, which can be triggered by surface doping. A Fermi surface yielding an appropriate nesting vector is identified by photoemission. Furthermore, a Br-induced lowering of Pt d-bands is observed, which accounts in part for the halogen-induced poisoning. The Pt–Br bond is shown to be essentially covalent, ruling out electrostatic poisoning mechanisms. © 2000 Elsevier Science B.V. All rights reserved.

**Keywords:** Angle resolved photoemission; Bromine; Chemisorption; Density functional calculations; Platinum; Scanning tunneling microscopy; Surface chemical reaction; Surface structure, morphology, roughness, and topography

In heterogeneous catalysis the adsorption of halogens is known to effectively inhibit several catalytic processes and to promote others [1]. Basically, the poisoning mechanisms proposed so far may be classified as predominantly covalent or primarily electrostatic interactions, respectively. Examples of the former category include a reduction of the density-of-states (DOS) at  $E_F$  caused by the ‘bonding-away’ of metal states into strongly bonding orbitals far below and strongly antibonding orbitals far above  $E_F$  upon halogen adsorption [2]. A closely related mechanism of this type was proposed recently by Hammer et al. [3–5]. They demonstrated a correlation between the position

of the metal d-band centroid with respect to  $E_F$  and the reactivity of the metal. Accordingly, lowering of the d-band centroid by adsorption of halogens should reduce the reactivity and give rise to a poisoning effect. The electrostatic mechanism, in contrast, is based on the assumption of a strongly ionic halogen–metal bond. The associated dipole moment has the opposite orientation of the one generated by alkali metal adsorption. Hence, the electrostatic field tends to withdraw electrons from a coadsorbate. Usually, the highest occupied orbitals of adsorbed molecules are derived from the lowest unoccupied molecular orbitals (LUMOS) of the free molecule, which become broadened and partially occupied upon interaction with the substrate. In general, the LUMO is antibonding with respect to the intramolecular bond. If charge is withdrawn from these orbitals, dissociation is inhibited and catalytic poisoning results

\* Corresponding author. Fax: +43-512-507-2925.

E-mail address: erminald.bertel@uibk.ac.at (E. Bertel)

<sup>1</sup> Permanent address: Infineon Technologies AG, Otto-Hahn-Ring 6, D-81739 Munich, Germany.

for reactions, where dissociation is the rate limiting step. Alternatively, the electrostatic interaction with the halogen could drive up the total energy of the transition state to dissociative adsorption. This is the reverse of a mechanism proposed by Mortensen et al. [6] for the alkali metal promoted dissociation of  $N_2$  on Fe.

An appraisal of the poisoning mechanisms sketched above requires detailed information on the adsorption geometry [1,7–9] and the electronic structure [10,11] of adsorbed halogens. The majority of the geometry studies are based on qualitative low energy electron diffraction (LEED) data. In several cases it is therefore unknown whether the observed structures correspond to simple adsorption systems or not. In view of the notorious reactivity of halogens, reconstruction and surface compound formation are realistic alternatives. Thus, the present combined LEED, scanning tunneling microscopy (STM) and angle resolved UV photoemission spectroscopy (ARUPS) study aims at a more rigorous characterization of the adsorption geometry and the ensuing electronic structure of adsorbed halogens.

At room temperature Br adsorbs molecularly on the close-packed rows of Pt(110) (the molecular adsorption will not be discussed further here). The Br molecules are imaged as holes with a depth of  $0.6 \text{ \AA}$  in the STM. Evidence for the molecular adsorption arises from the fact that, upon annealing to beyond 420 K, these ‘holes’ decay into twice the number of indentations with a depth of  $0.2 \text{ \AA}$ . The latter occur almost invariably as pairs, exhibiting a separation of  $5.54 \text{ \AA}$ . Fig. 1 shows such an STM image recorded at Br coverages of a few per cent after annealing. The areal density of the indentations corresponds rather precisely to the Br coverage determined from temperature programmed desorption (TPD). Accordingly, we interpret the pairwise indentations as Br atoms adsorbed in next-nearest neighbour (nnn) sites. It is noteworthy that the Br atom pairs almost exclusively occupy nnn sites, indicating a very efficient dissipation of the energy liberated upon dissociative adsorption. This is in marked contrast to the behaviour observed on semiconducting substrates [12]. The fact that Br atoms (and molecules) appear as ‘holes’ rather than protrusions parallels

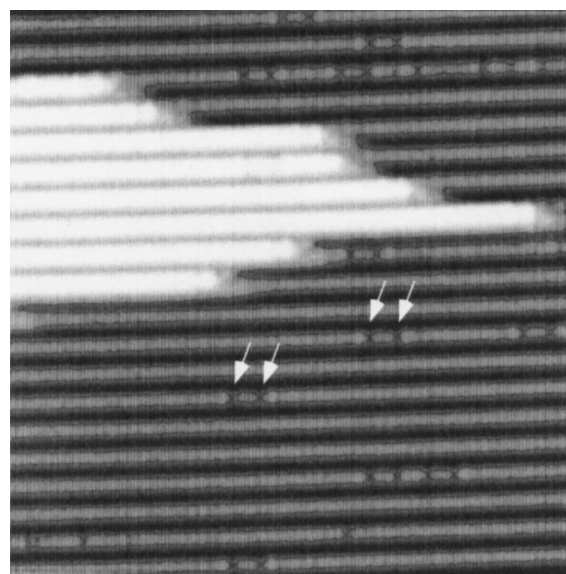
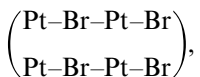


Fig. 1. STM constant current map ( $145 \times 145 \text{ \AA}^2$ ) of Pt(110)- $(1 \times 2)$  with a bromine coverage  $\theta_{Br} \approx 0.02 \text{ ML}$ . The bright area is an upper terrace separated from the lower terrace by a monatomic step with a high kink density. The latter originates from the strongly anisotropic step energies characteristic of the Pt(110)- $(1 \times 2)$  surface. The bromine atoms are imaged as indentations (see arrows) in the close-packed rows. Note that these indentations occur almost exclusively in pairs, separated by a distance of  $5.54 \text{ \AA}$ .

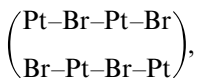
the behaviour of oxygen and is generally attributed to a lowering of the local DOS at the Fermi level near the adsorbed species.

Upon further  $Br_2$  exposure an increasing number of protrusions appear in the troughs of the missing row reconstructed surface. Again, the distance between these protrusions is  $5.54 \text{ \AA}$ . The morphology of Pt atoms sandwiched between two Br atoms in the close-packed rows, and of the protrusions appearing in the trenches, is indistinguishable. Accordingly, we identify the latter with Pt atoms. Hence, at coverages beyond a few per cent, annealing to 420 K causes nucleation of Pt–Br–Pt chains within the close-packed rows as well as within the troughs. The Pt atoms required for nucleation of the chains in the troughs are delivered from the substitutional adsorption of Br in the close-packed rows. As these nuclei grow into extended chains, the missing rows are filled in

and, depending on the phase shift between neighbouring chains, local  $p(2 \times 1)$ , i.e.



or  $c(2 \times 2)$  structures, i.e.



are formed. For  $\theta_{\text{Br}} < 0.5$  ML (monolayers) both structures are observed with almost equal probability. This near-degeneracy of the two structures suggests a weak chain–chain interaction compared with the intra-chain interaction. In particular, it argues against an ionic character of the Pt–Br bond, because in that case the  $c(2 \times 2)$  structure should be strongly preferred. At precisely 0.5 ML coverage, the  $c(2 \times 2)$  structure dominates [close to defects or steps the  $p(2 \times 1)$  structure is still observable]. The  $c(2 \times 2)$  layer is stable up to 780 K.

Desorption of a few per cent of Br from the

$c(2 \times 2)$  structure causes entire sections of the Pt–Br–Pt chains to be removed out of the layer and to be reassembled as added rows on top of it (Fig. 2). This underlines the strong anisotropy of the bonding interactions within the Pt/Br layer. Accordingly, the Pt–Br surface compound can be most appropriately envisioned as a 2D array of quasi-1D Pt–Br–Pt chains. This is reminiscent of the well-known tendency of Pt–halogen compounds to form halogen-bridged linear chain molecules [13]. Quasi-1D systems in general tend to exhibit a strong electron–phonon coupling, giving rise to Kohn anomalies or even the occurrence of a charge density wave (CDW) ground state [14]. In fact, the halogen-bridged transition-metal linear chain compounds attracted considerable interest on account of their ability to be tuned into different ground states, for instance CDW or spin density wave ground states, by pressure, temperature, chemical substitution or doping. A critical property determining the response of the charge distribution to lattice distortions and vice versa is the so-called Fermi surface nesting, i.e. the extent of parallel sections of the Fermi surface in  $k$ -space which can be connected by the same wave vector

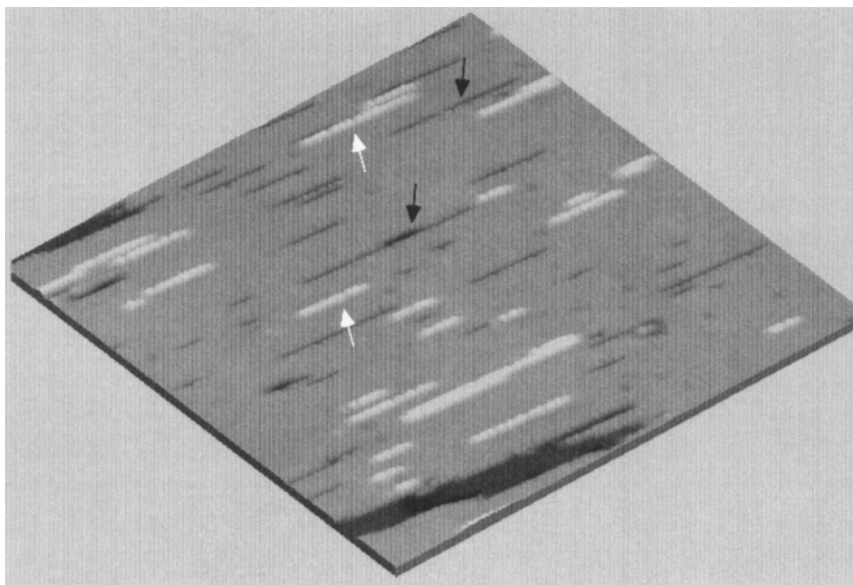


Fig. 2. STM constant current map ( $420 \times 420 \text{ \AA}^2$ ) of Br/Pt(110) with  $\theta_{\text{Br}} \approx 0.48$  ML. Entire sections of the Pt–Br–Pt chains are expelled (see e.g. black arrows) from the Pt(110)/Br- $c(2 \times 2)$  layer and form added rows (white arrows). The strongly anisotropic interactions within the layer result in a one-dimensionally disordered surface for  $\theta_{\text{Br}} = 0.5 - \delta$  ML.

$q$ . For the present system, the electronic structure was investigated theoretically by self-consistent, full-potential linearized augmented plane-wave (FLAPW) model band structure calculations carried out with the WIEN95 program package [15,16]. In a first approach, the band structure was calculated for a free-standing Pt/Br- $c(2 \times 2)$  monolayer. In the  $\bar{\Gamma}\bar{X}$  azimuth [ $(1\bar{1}0)$  direction] the bands exhibit strong dispersion consistent with a strong intra-chain interaction, while the weak dispersion found in the  $\bar{\Gamma}\bar{Y}$  azimuth [ $(001)$  direction] parallels the weak inter-chain interaction observed experimentally. In the model calculation the Fermi energy is located in a gap between the antibonding  $\pi$ -manifold and the antibonding  $\sigma$  band. Assuming that the Fermi level can be tuned by doping with acceptors to eventually fall within the  $\pi$ -manifold, one can map out the corresponding Fermi surfaces. Due to the 1D character of the bands the resulting Fermi contours are found to be essentially flat, thus allowing the pronounced Fermi surface nesting required for the stabilization of a CDW ground state.

Experimentally, the doping with acceptor

species is realized by a slight exposure of the  $c(2 \times 2)$  layer to  $\text{Br}_2$ , leading to a coverage of  $\Theta_{\text{Br}} = 0.5 + \delta$  ML, where the excess coverage  $\delta$  is of the order of  $10^{-3}$  (!). After exposure at room temperature the  $\text{Br}_2$  molecules adsorb randomly on the  $c(2 \times 2)$  layer (Fig. 3). The STM image shows each doping molecule to be surrounded by a plane-wave domain with a corrugation of  $\sim 0.3$  Å and a periodicity corresponding to three nn distances of the Pt substrate. The wavefronts are perpendicular to the  $(1\bar{1}0)$  direction. Hence the corresponding wave vector  $q$  is parallel to the close-packed rows. Although superficially reminiscent of Friedel oscillations around defects observed previously [17], these waves are of different origin for several reasons: their corrugation is an order of magnitude higher than that associated with Friedel oscillations; the periodicity of the observed wave-pattern is independent of the tunneling bias; and the periodicity of the waves is picked up in LEED giving rise to  $1/3$  spots. The only explanation consistent with the whole body of experimental results is the formation of CDW domains around the doping molecules. This interpretation

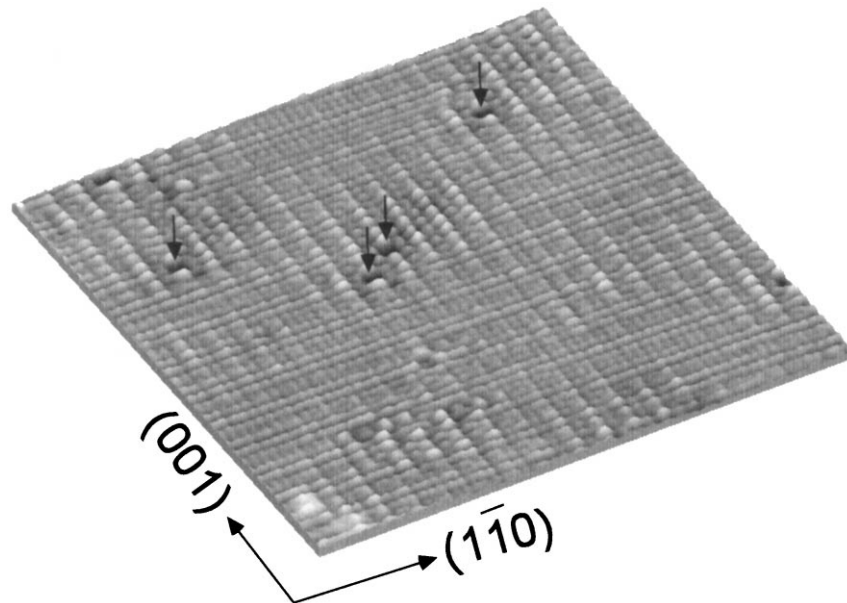


Fig. 3. STM constant current map ( $150 \times 150$  Å<sup>2</sup>,  $U_{\text{bias}} = -100$  meV) of a Pt(110)/Br- $c(2 \times 2)$  layer doped with about 0.005 ML of bromine. The doping particles are imaged as deep holes (arrows). Around each particle, a charge density wave domain with three-fold periodicity along the  $(1\bar{1}0)$  direction is formed. The domains are not in phase and therefore interfere destructively in some areas.

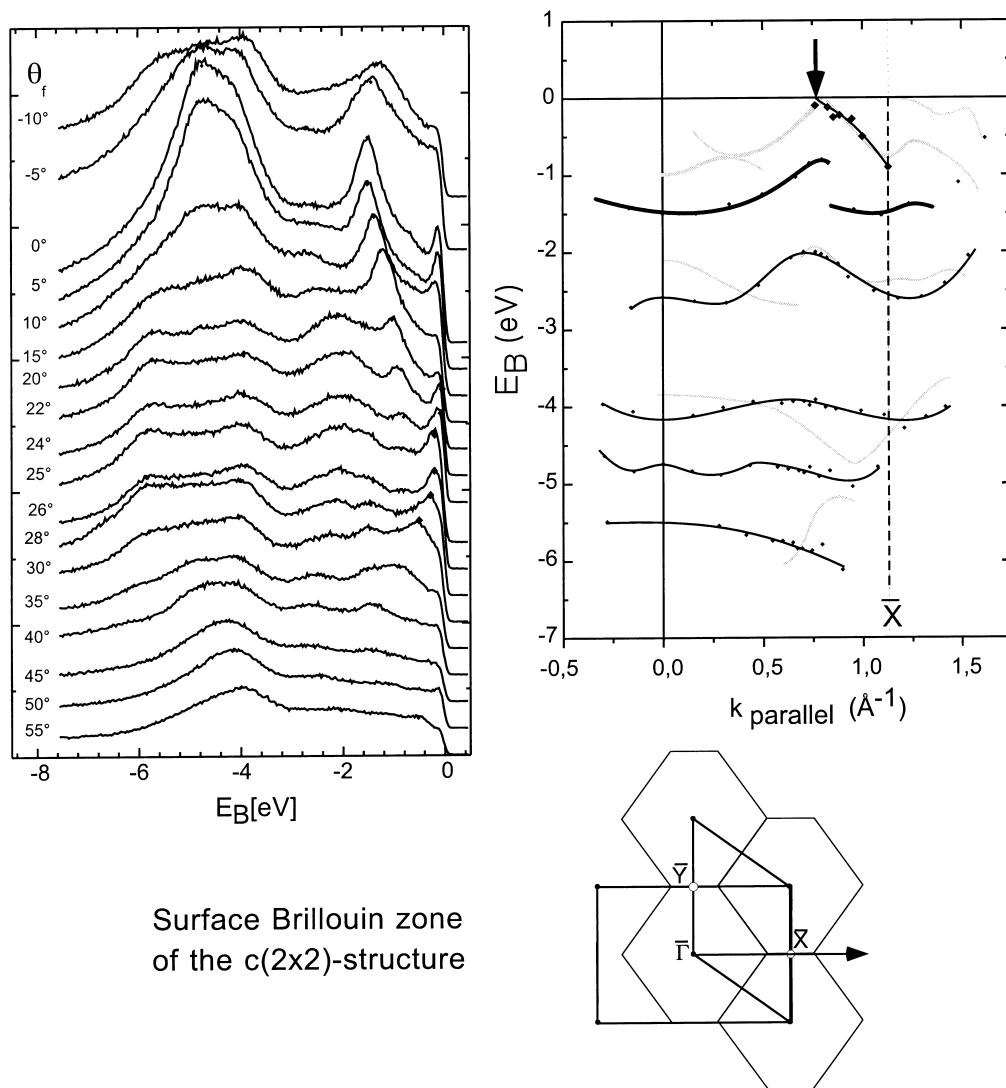


Fig. 4. Left panel: photoemission spectra (HeI) of the Pt(110)/Br- $c(2 \times 2)$  layer for different electron emission angles. Right panel: peak energies  $E(k_{\parallel})$  derived from the ARUP spectra (dots and black lines). Note the Fermi level crossing at  $k = 0.75 \text{ \AA}^{-1}$  (arrow). For comparison, the dispersion of ARUPS features  $E(k_{\parallel})$  for clean Pt(110) is shown as grey lines. Some of the bands near  $E_F$  appear to be downshifted after Br adsorption (marked by heavy lines). Bottom panel: the rectangular surface Brillouin zone (SBZ) for Pt(110)-(1  $\times$  1) and the 'distorted hexagonal' SBZ for Pt(110)/Br- $c(2 \times 2)$ , respectively.

is supported by the fact that slight annealing of the structure shown in Fig. 3 leads to the formation of a perfect  $(3 \times 1)$  LEED pattern and an STM image, where the individual domains disappear in favour of a perfectly ordered global structure with three-fold periodicity in  $(1\bar{1}0)$  direction. This is in

precise agreement with the properties of a global, commensurate CDW phase.

To further explore the unusual properties of the Pt/Br surface compound, ARUP spectra were measured. Fig. 4 (left panel) shows the spectra measured along the  $\bar{\Gamma}\bar{X}$  azimuth, while in Fig. 4 (right

panel) the dispersion of the bands in the  $c(2 \times 2)$  structure is compared with the dispersion found for the clean Pt(110)- $(1 \times 2)$  surface. In the present context two features are relevant. First, a Fermi level crossing is found at  $k \approx 0.75 \text{ \AA}^{-1}$ . This yields  $q = 2k_F - G = 1.50 - 2.27 = -0.76 \text{ \AA}^{-1} \approx -G/3$ , where  $G$  is the length of a reciprocal lattice vector in the  $\bar{\Gamma}\bar{X}$  azimuth. Thus,  $q$  is just the nesting vector needed to produce a CDW with three-fold periodicity.

The second significant feature in Fig. 4 is the appearance of Br related bands at 1–1.5 eV below  $E_F$ . At least one of these bands parallels the dispersion of a band observed on the clean Pt surface between  $-1 \text{ eV}$  and  $E_F$  (these bands are shown as heavy lines). The Br-induced downshift of metal d-states suggested by this observation should cause a reduction of the reactivity of this system [3–5]. Furthermore, if the system is driven into the CDW ground state, the Peierls distortion associated with the CDW opens a gap at  $E_F$ , the so-called Peierls gap. As the CDW is stable at room temperature, the gap has to be of the order of 100 meV [14]. The opening of the Peierls gap is therefore associated with a *global* decrease of the DOS in a considerable energy interval around  $E_F$ . This should reduce the reactivity of the system even further. It is to be noted, however, that a decrease of the *local* DOS around adsorbed Br is indicated by the STM topographic contrast — remember that the Br atoms appear as holes — even at very low coverages in the normal ground state of the adsorbate–substrate system.

In summary, a halogen-induced reconstruction in the system Br/Pt(110) leads to the formation of a 2D array of quasi-1D Pt–Br–Pt chains, which may be considered as a surface analogue of the halogen-bridged transition-metal linear chain compounds. The 1D character of the surface compound is demonstrated not only by the morphology of the defective layer ( $\Theta_{\text{Br}} = 0.5 - \delta \text{ ML}$ ), but also by the appearance of a CDW ground state in the doped layer ( $\Theta_{\text{Br}} = 0.5 + \delta \text{ ML}$ ). The strong directionality of the metal–halogen bond argues in favour of predominantly covalent bonding. For this reason, and in view of the observed substitu-

tional adsorption geometry, electrostatic effects on coadsorbates can be expected to be insignificant on such a surface. The poisoning is therefore attributed to covalent mechanisms, namely a halogen-induced lowering of the metal d-band centroid, a depletion of the local DOS at  $E_F$  near adsorbed halogen species and, in the case of the CDW ground state, a global depletion of the DOS at  $E_F$ .

## Acknowledgements

Support by the Austrian Science Fund is gratefully acknowledged. The work of UB was supported by the Deutsche Forschungsgemeinschaft through SFB 338.

## References

- [1] R.G. Jones, Progr. Surf. Sci. 27 (1988) 25.
- [2] M.P. Kiskinova, Poisoning and Promotion in Catalysis Based on Surface Science Concepts and Experiments, Elsevier, Amsterdam, 1992.
- [3] B. Hammer, Y. Morikawa, J.K. Nørskov, Phys. Rev. Lett. 76 (1996) 2141.
- [4] B. Hammer, J.K. Nørskov, Surf. Sci. 343 (1995) 211.
- [5] B. Hammer, M. Scheffler, Phys. Rev. Lett. 74 (1995) 3487.
- [6] J.J. Mortensen, B. Hammer, J.K. Nørskov, Phys. Rev. Lett. 80 (1998) 4333.
- [7] E. Bertel, F.P. Netzer, Surf. Sci. 97 (1980) 409.
- [8] H. Gutleben, E. Bechtold, Surf. Sci. 236 (1990) 313 and references cited therein.
- [9] R.G. Jones, M. Kadodwala, Surf. Sci. 370 (1997) L219.
- [10] H. Hinzert, K.K. Kleinherbers, E. Janssen, A. Goldmann, Appl. Phys. A 49 (1989) 313 and references cited therein.
- [11] G.N. Kastanas, B.E. Koel, Appl. Surf. Sci. 64 (1993) 235.
- [12] U. Diebold, W. Hebenstreit, G. Leonardelli, M. Schmid, P. Varga, Phys. Rev. Lett. 81 (1998) 405.
- [13] M. Alouani, J.W. Wilkins, R.C. Albers, J.M. Wills, Phys. Rev. Lett. 71 (1993) 1415 and references cited therein.
- [14] S. Kagoshima, H. Nagasawa, T. Sambongi, One-Dimensional Conductors, Springer, Berlin, 1988.
- [15] P. Blaha, K. Schwarz, P. Dufek, R. Augustyn, WIEN95, Technical University of Vienna, 1995.
- [16] P. Blaha, K. Schwarz, P. Sorantin, S.B. Trickey, Comput. Phys. Commun. 59 (1990) 399.
- [17] M.F. Crommie, C.P. Lutz, D.M. Eigler, Science 262 (1993) 218.